IEEE Access
Multidisciplinary | Rapid Review | Open Access Journal

Received December 22, 2017, accepted January 14, 2018, date of publication January 17, 2018, date of current version March 9, 2018.

Digital Object Identifier 10.1109/ACCESS.2018.2794606

Compact, Printed, Tri-Band Loop Antenna With Capacitively-Driven Feed and End-Loaded Inductor for Notebook Computer Applications

SAOU-WEN SU[1], (Senior Member, IEEE), CHENG-TSE LEE[1], (Member, IEEE), AND SHU-CHUAN CHEN[2], (Member, IEEE)

[1]Antenna Design Department, Advanced EM and Wireless Communication Research and Development Center, ASUS, Taipei 11259, Taiwan
[2]Department of Electrical and Electronic Engineering, Chung Cheng Institute of Technology, National Defense University, Taoyuan County 33551, Taiwan

Corresponding author: Saou-Wen Su (Saou-Wen_Su@asus.com)

ABSTRACT The shorted monopoles and the planar inverted-F antennas have been utilized for wireless local area network (WLAN) notebook applications for years. This paper presents an alternative and yet promising antenna type with a compact and smaller size of 5 mm × 20 mm to operate in the 2.4 GHz (2400–2484 MHz), 5.2 GHz (5150–5350 MHz), and 5.8 GHz (5725–5825 MHz) WLAN bands. The loop antenna, formed on a 0.4-mm-thick FR4 substrate, was adopted in this study. The loop radiator comprised a capacitively-driven feed and an end-loaded inductor. The capacitively-driven feed allowed the antenna to generate the quarter-wavelength loop resonance for possible lowest resonant mode excitation in addition to the loop's half-wavelength mode. By loading an inductor at the loop end to be connected to the small antenna ground, the operating frequencies of the quarter- and half-wavelength resonances were further decreased to cover the 2.4 and 5.2/5.8 GHz bands with good input impedance therein.

INDEX TERMS Loop antennas, notebook computer antennas, wireless local area network (WLAN) antennas, quarter-wavelength loop resonance.

I. INTRODUCTION

For mobility and productivity, notebook computers have been favored by many end users in various fields. For stable wireless connection and better signal coverage, the antenna plays a crucial role in the designs of notebook computers. The best antenna location based on the results from our empirical investigation is along the top edge above the notebook display mainly because the antenna radiation patterns are mostly omnidirectional, providing good wireless coverage, and the antennas are also away from the system-level noise with less radio frequency interference (RFI) problems. Many promising antennas placed above the top edge of the notebook display for wireless local area network (WLAN) notebook applications have been reported in [1]–[16]. These include the designs of the shorted monopoles and planar inverted-F antennas (PIFAs) [1]–[6], the coupled-fed monopole and PIFAs [7]–[11], the monopole [12] and the dipole [13] antennas, the slot antennas [14]–[16], and so on. Except for the slot antennas, which operate at their half-wavelength resonant mode [14]–[16], those quarter-wavelength antennas studied in [1]–[12] generally require a planar design area of width (antenna height) larger than 5 mm or lateral length larger than 30 mm.

To embrace Gbps data rate with higher through-put performance, 4 × 4 WLAN antennas embedded in the notebook computers can be foreseen in the near future. This will create more challenges for antenna engineers because antenna real estate is already a very limited commodity for current large screen-to-body-ratio notebooks. In order to deploy more antennas, the single antenna itself must be even smaller and yet does not compromise on its antenna performance. To meet this requirement, a novel printed antenna with a small design footprint of area 5 mm × 20 mm only is proposed. To the authors' best knowledge, the proposed design footprint (100 mm^2) is so far the smallest among the conventional notebook antennas for 2.4/5.2/5.8 GHz, tri-band WLAN operation (refer to Table 1 for comparison). In Table 1, only the antennas in planar structure (no three-dimensional structure, for example the design in [6]) and operating at the quarter-wavelength resonant mode are listed. Notice that in [7],

TABLE 1. Comparison of the planar antennas for notebook applications with regard to the covered operating bands and the overall occupied antenna area.

Ref.	Operating bands	Area of width (height) × length
1	2.4/5.2/5.8 GHz*	values not given
2	2.4/5.2/5.8 GHz	4 mm × 38.5 mm**
3	2.4/5.2 GHz*	12 mm × 54 mm
4	2.4/5.2/5.8 GHz	5 mm × 37.5 mm**
5	2.4/5.2/5.8 GHz	5 mm × 35 mm
7	5.2/5.8 GHz	5 mm × 12.5 mm**
8	2.4/5.2/5.8 GHz	6 mm × 20 mm**
9	2.4/5.2/5.8 GHz, 2.5/3.5/5.5 GHz	12 mm × 13 mm
10	2.27-11 GHz	12 mm × 13.75 mm**
11	2.4/5.2/5.8 GHz	18 mm × 7 mm
12	2.4/5.2/5.8 GHz	8.7 mm × 5.4 mm**
proposed	2.4/5.2/5.8 GHz	5 mm × 20 mm

*High-band bandwidth not completely covered
**No antenna ground concerned for feeding cable; antenna width will be larger in applications

the obtained impedance bandwidth defined by 10-dB return loss can not cover WLAN operation in the 2.4 GHz band (only 5.2/5.8 GHz bands achieved).

The antenna type in this study is different from those conventional notebook computer antennas presented in [1]–[16]. In this paper, the loop design was adopted to achieve the small-sized WLAN antenna for practical notebook applications. Loop and folded loop antennas have been favorable to applications in WLAN access points and mobile phones owing to their inherent self-balanced structure (one-wavelength loop) [17]–[23] and offering multi-resonant modes [24]–[28]. Loop antennas usually operate at their half-, one-, and one-half-wavelength resonant modes and can also operate at the quarter-wavelength resonant mode for size reduction [29], [30]. However, very scant loop designs have been applied to the notebook computers.

The proposed loop antenna was formed on a dielectric substrate and comprised an L-shaped loop radiator and a small antenna ground. The length of the L-shaped loop was about 17 mm (about 0.14-wavelengths in free space at 2445 MHz) and fed at one end of the loop with a chip inductor loaded at the opposite end to short-circuit the loop. The antenna ground was reserved in the design footprint for grounding the antenna cable, which is not allowed to be placed behind the display in the real notebook computer owing to the concern for the back pressure created on the display. The capacitively-driven feed was inserted at a small distance to the feed port and had an S-shaped coupling gap. The driven feed had similar effects to those of the coupling strip in [29], which helps the loop generate the quarter-wavelength resonant mode. By loading the inductor at the loop end to connect to the antenna ground, the operating frequencies of the quarter- and the half-wavelength modes were further decreased to cover the 2.4 and 5.2/5.8 GHz bands. The proposed antenna was first analyzed in the simulation and validated by measurement. Details of the antenna design are described, and the results thereof are described and discussed in the paper.

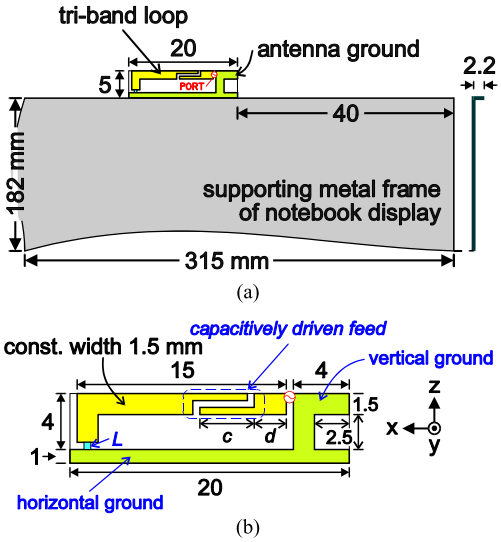

FIGURE 1. (a) Configuration of the proposed, tri-band loop antenna affixed to the supporting metal frame of a 14-inch notebook display. (b) Detailed dimensions of the printed loop antenna.

II. PROPOSED COMPACT LOOP ANTENNA

A. ANTENNA CONFIGURATION AND DESIGN CONSIDERATION

Fig. 1(a) illustrates the proposed loop design set above the top edge of the supporting metal frame of the notebook display. The design was constructed on a single-layered, flame retardant 4 (FR4) substrate ($\varepsilon_r = 4.4$) of size 5 mm × 20 mm and comprised an L-shaped loop radiator and a small antenna ground. The metal frame is of a 14-inch display measuring 2.2 mm × 182 mm × 315 mm and can be regarded as the large system ground for the antenna and the electromagnetic interference (EMI) grounding. A 1.0-mm-thick stainless-steel plate, coated with the zinc for solderability, was utilized for the metal frame in the experiments. The antenna substrate was located in the narrow bezel of the display and spaced 40 mm apart from the right side corner. For practical applications, this 40 mm clearance area is reserved for mechanical structures for assembly, not available for antenna placement.

Fig. 1(b) details the parameters of the design prototype. The loop radiator and its ground plane formed a compact rectangular structure. The loop radiator occupied an area of 4 mm × 15 mm and had a constant strip width of 1.5 mm. The antenna feed port was placed at one end of the loop 5 mm above the frame, and the chip inductor was loaded at the opposite end to short-circuit the loop. Notice that this arrangement of the feed port can be required by some practical cases that the antenna feeding cable is routed along the top edge of the notebook cover therein. The small antenna ground comprised horizontal and vertical portions. For practical applications, the grounding copper tape was used to connect the antenna ground to the display metal frame, and thus, the horizontal ground portion was reserved on the antenna substrate. As for the vertical ground portion, a tiny square of size 2.5 mm × 2.5 mm was cut in the ground (L-shaped ground) for better impedance bandwidth in the 5 GHz band (see Fig. 5). A short,

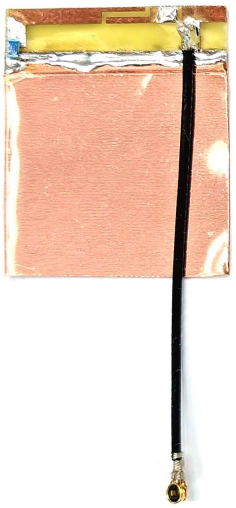

FIGURE 2. Photo of the prototype made of a 0.4-mm-thick FR4 substrate and fed by a 50-Ω mini-coaxial cable of length 40 mm.

50-Ω mini-coaxial cable of length 40 mm was used to test the loop across the feed gap of 0.5 mm. In this case, the vertical ground portion also provided the grounding area for the outer shielding of the feeding cable (see Fig. 2).

The capacitively-driven feed was inserted at a small distance of d to the feed port and had an S-shaped coupling gap of 0.5 mm. The length of the coupling gap was the sum of the loop-radiator strip width 1.5 mm and the driven feed length c. This capacitively-driven feed helped generate the quarter-wavelength loop resonance in addition to the loop's half-wavelength resonant mode. By furthermore loading the series-connected inductor at the loop end between the loop radiator and the horizontal ground, the operating frequencies of the quarter- and the half-wavelength loop modes can be decreased to cover the 2.4 and 5.2/5.8 GHz bands. With the proper selections of the parameters d, c of the capacitively-driven feed and the inductor values, tri-band WLAN operation with good impedance matching can be achieved. The near optimum parameters in this design were obtained using the ANSYS HFSS [31]. Notice that the length of the L-shaped loop radiator was about 17 mm, which corresponded to about 0.14- and 0.31-wavelengths in free space at 2445 and 5415 MHz, respectively, for the designed lower and upper bands. The decreased resonant lengths are caused by the end-loaded inductor, which provides additional inductance to compensate for large capacitance resulting from decreased operating frequencies [see Fig. 4(b)] [32].

B. OPERATING PRINCIPLE

A simple, L-shaped loop (Ant1) and the loop with the capacitively-driven feed (Ant2) [see insets in Fig. 3(a)] were first analyzed. The simulated return loss and the input impedance are shown in Fig. 3; the dimensions are kept the same as those in Fig. 1. It is first seen that a single resonance at 7070 MHz is generated for Ant1. This resonant mode represents the typical fundamental mode of the half-wavelength loop resonance. For Ant2, the additional lower-

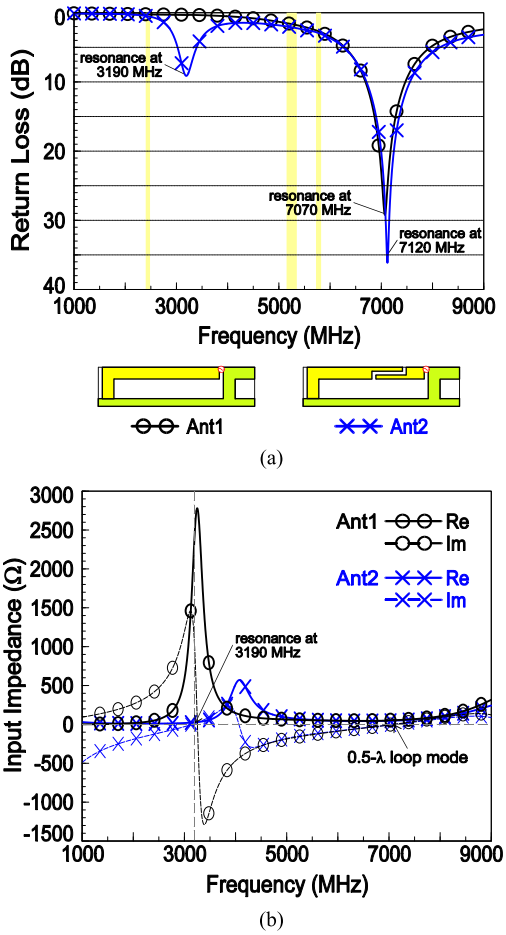

FIGURE 3. Simulated (a) return loss and (b) input impedance for the simple L-shaped loop (Ant1) and the loop with the capacitively-driven feed (Ant2; $d = 2$ mm, $c = 3.9$ mm).

band resonance at 3190 MHz can be generated with the upper-band resonance slightly shifting to 7120 MHz. That's, two resonances for Ant2 are obtained. For the simple loop (Ant1), very large inductance of about 2300 Ω and resistance of about 1120 Ω with the anti-resonance at about 3.2 GHz are seen in the lower band in Fig. 3(b), making the loop non-responsive for lower-band operation. With the presence of the capacitively-driven feed, large inductance and resistance can be mitigated (inductance reduced to about 9 Ω; resistance about 25Ω for Ant2), allowing the loop to acquire the additional, quarter-wavelength resonance in the lower band. Over the 5-9 GHz frequencies, the characteristics of the input impedance are similar between Ant1 and Ant2, and for reasons of that, the occurrence of the half-wavelength loop resonance is less affected.

Fig. 4(a), (b) shows the simulated return loss and the input impedance for Ant2 and the proposed loop (Ant2 with end-loaded inductor). It can be found in Fig. 4(a) that the operating frequencies of the two resonant modes over the lower and the upper bands are largely decreased for Ant2 with the series-connected inductor at the loop end. In this case, the desired WLAN bands for 2.4, 5.2, and 5.8 GHz operation can be achieved for the proposed design. The chip inductor

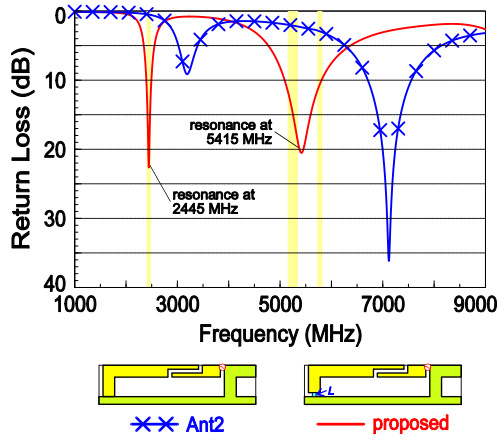

(a)

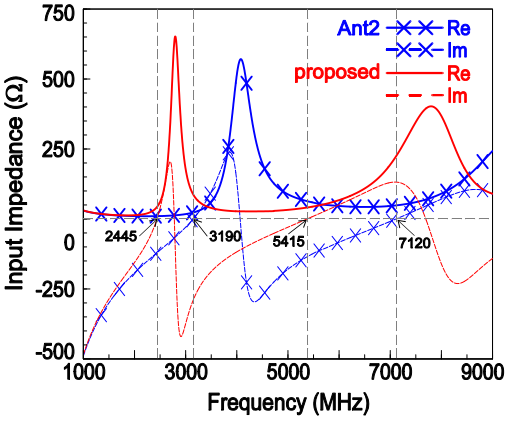

(b)

FIGURE 4. Simulated (a) return loss and (b) input impedance for Ant2 and the proposed loop (Ant2 with end-loaded inductor; $d = 2$ mm, $c = 3.9$ mm, $L = 4.7$ nH).

here can increase the electrical length of the L-shaped loop, thereby providing the antenna to gain extra resonant path for achieving decreased operating frequencies. In Fig. 4(b), the half-wavelength loop mode of Ant2 shifts toward the lower frequencies from 7120 to 5415 MHz while the quarter-wavelength mode moves from 3190 to 2445 MHz. Notice that the reactance of the lower-band resonance becomes closer to 50 Ω level (from 25 to 45 Ω), and in turn better impedance matching can be observed. Fig. 5 shows the simulated return loss for the antenna design with the L-shaped, vertical ground (proposed) and with the rectangular, vertical ground (reference). For the reference, the frequencies of the 2.4 GHz band are almost the same with those for the proposed. However, for 5 GHz operation, the center frequency shifts from 5415 to 5605 MHz with a slight decrease in reactance (from 42 to 38 Ω; impedance results not shown for brevity). The results indicate that with a tiny cut in the vertical ground, the upper-band frequencies are decreased with better impedance matching.

III. EXPERIMENTAL AND SIMULATION RESULTS

Based on the antenna parameters discussed in Section II, a prototype of the proposed antenna as shown in Fig. 2 was

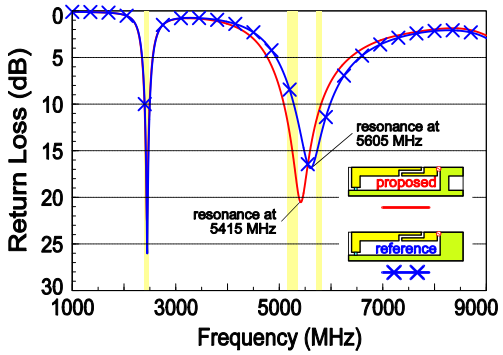

FIGURE 5. Simulated return loss for the design with the L-shaped, vertical ground (proposed) and with the rectangular, vertical ground (reference; no cut in ground).

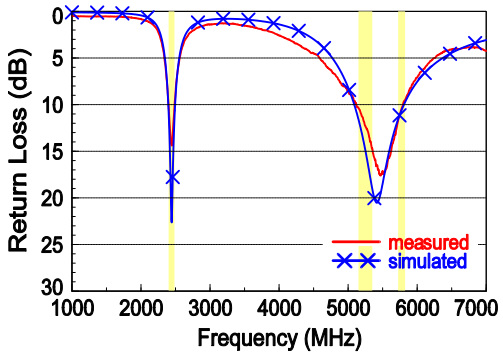

FIGURE 6. Measured and simulated return loss for the proposed antenna; $d = 2$ mm, $c = 3.9$ mm, $L = 4.7$ nH.

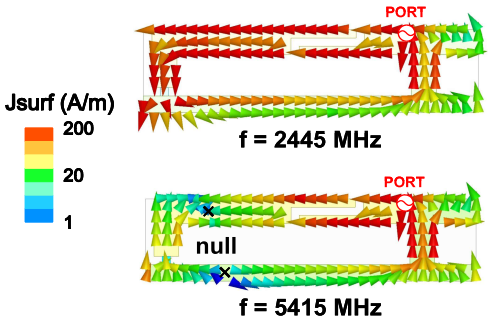

FIGURE 7. Simulated surface currents in the form of vectors excited at 2445 and 5415 MHz for the antenna studied in Fig. 6.

constructed and tested. Fig. 6 shows the measured and the simulated return loss for the design prototype. The two resonant modes for the lower and the upper bands are excited. The experimental data compare favorably with the simulation results, which were calculated using the finite element method [31]. The shaded frequency ranges mark the 2.4, 5.2, and 5.8 GHz WLAN bands. The measured impedance matching over the lower and the upper resonant modes all exceeds the 10-dB return loss, which satisfies the matching and bandwidth specification for WLAN operation.

The studies of the antenna surface-current distributions are presented in Fig. 7. Two resonant modes excited at 2445 and 5415 MHz (most matched frequency points in simulation) were chosen to help illustrate the operating principle of the

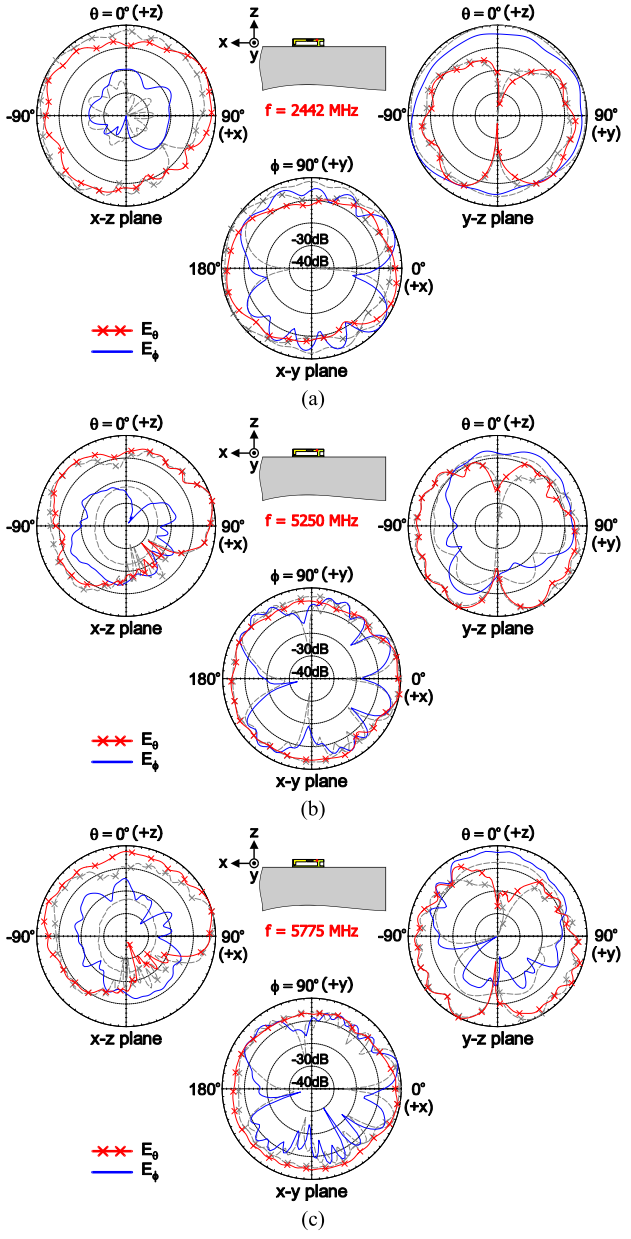

FIGURE 8. Measured and simulated radiation patterns of the proposed antenna at (a) 2442 MHz, (b) 5250 MHz, and (c) 5775 MHz.

design. The currents are plotted in the form of vectors using arrow shape. For the lower band at 2445 MHz, the surface currents are seen mostly populated on the loop radiator and its small ground (image currents) with no current nulls spotted, which confirms that the quarter-wavelength loop resonance is generated. For frequencies in the upper band, it can be seen that at 5415 MHz, one current null denoted by a cross is found on the loop radiator. This indicates that the upper-band resonance is of a half-wavelength loop mode. Notice that the location of this current null occurs not in the middle of the loop's strip path. This property is expected because the chip inductor increases the electrical length of the loop, as described in Section II, which shifts the null toward the end of the L-shaped loop.

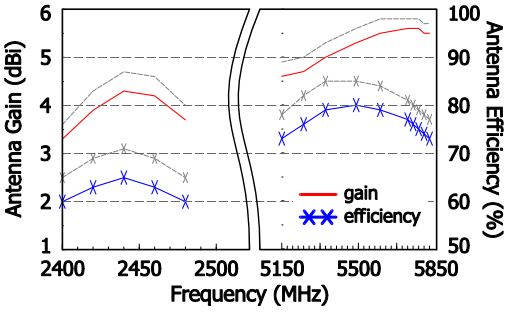

FIGURE 9. Measured and simulated peak antenna gain and antenna efficiency for the antenna studied in Fig. 8.

The over-the-air (OTA) performance of the design in free space was studied. The measurement was taken at the 4 m × 4 m × 4 m, SATIMO chamber using the conical-cut method [33]. Fig. 8(a)–(c) shows the measured and the simulated, far-field radiation patterns at 2442, 5250, and 5775 MHz, the center frequencies of the 2.4, 5.2, and 5.8 GHz bands. The simulated patterns are shown in gray dash lines. The discrepancies are due to the measurement tolerance and cable effects (no cable in simulation). The patterns plotted here were normalized with respect to the maximum field strength in each cut. The omnidirectional radiation patterns are observed in the x-y planes over the bands (see E_θ fields) with larger radiation toward the $+z$ direction in the elevation planes above the display's metal frame. The radiation characteristics are also similar to those of the WLAN notebook computer antennas in [1]–[11]. Good consistency in the patterns over the bands (compared with other in-band frequencies measured) was also obtained. Fig. 9 plots the measured and the simulated, peak antenna gain and antenna efficiency against frequency for the proposed antenna. The simulation results are indicated by gray lines. The measured peak gain in the 2.4 GHz band is the range of 3.4 to 4.2 dBi with efficiency exceeding 60%. For 5.2/5.8 GHz bands, the gain varies from 4.7 to 5.6 dBi with efficiency in the range of 74% to 79%. The simulated antenna efficiency and peak gain are larger than the measured data by 6% and 0.4 dBi as maximum. Notice that the OTA measurement here takes account of the mismatch loss of the antenna; the realized gain [34] and the antenna efficiency [35] were measured.

IV. PARAMETRIC STUDIES

Among a few antenna parameters that affect the antenna operating frequencies, three parameters are chosen here for further discussion. First, the effects of the location d and the length c of the capacitively-driven feed are looked into, and the results of the simulated return loss as a function of these two parameters are given in Fig. 10. In Fig. 10(a), the frequency ratio of the upper and the lower resonance is found to decrease from 2.4 (5690/2350 MHz) to 2.1 (5270/2495 MHz) when the value d increases from 1 to 3 mm with the impedance matching of the two resonant modes becoming poorer. In this case, the location d of 2 mm, which gives the frequency ratio of 2.2, is the near optimal value in this design. For the length

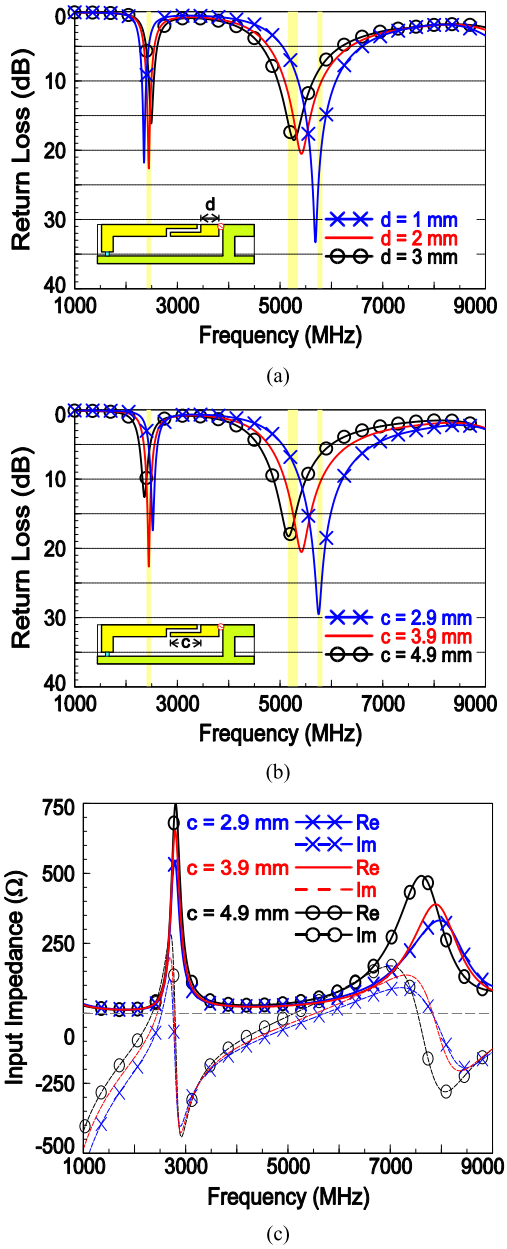

FIGURE 10. Simulated return loss for the proposed antenna as a function of (a) the location *d* and (b) the length *c* of the capacitively-driven feed, and (c) the input impedance for the length *c* of the capacitively-driven feed.

c of the capacitively-driven feed, it is seen that in Fig. 10(b), this parameter also affects the operating frequencies of the upper and the lower resonant modes but has less effects on the frequency ratio, compared with those of the location *d*. The characteristics of the input impedance over the 2-4 GHz frequencies are seen similar in Fig. 10(c) and show smaller reactance (less inductive) when the value *c* decreases. On the other hand, the input impedance over the 5-9 GHz frequencies varies with the length *c* (also less inductive with decreased values *c*). As a whole, the upper band is more affected because larger surface currents are distributed between the feed port and the capacitively-driven feed and also thereon (see Fig. 7). From the results, it can be concluded that the

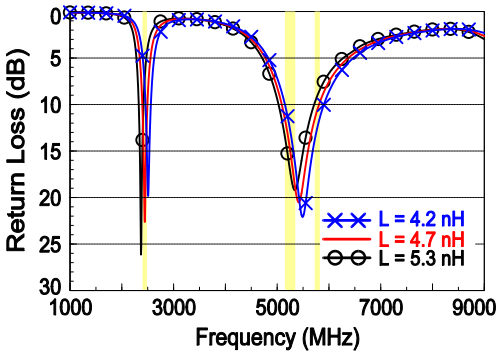

FIGURE 11. Simulated return loss for the proposed antenna as a function of the end-loaded inductor *L*.

location and the length of the driven feed can be used to fine-tune the desired frequency ratio of the upper and the lower resonance and the operating frequencies thereof with the overall design footprint fixed.

The other chosen parameter for the studies is the end-loaded inductor L. Fig. 11 shows the simulated return loss as a function of the chip inductor L; other dimensions are kept the same as studied in Fig 6. As mentioned in Section II, the inductor loaded between the loop end and the ground allowed the design to achieve further decreased operating frequencies. Thus, large inductor values of L can lead to lower frequencies of the proposed antenna, as seen from the results in Fig. 11. Notice that these inductor values used in the simulation were from the datasheet of the Murata LQW15A 0402 series. The impedance bandwidth for the cases of $L = 4.2$ nH to $L = 5.3$ nH are also not much changed for the upper and the lower bands with the frequency ratio of the two resonant modes kept about 2.2 (preferred ratio for this design). These properties provide antenna engineers an easier parameter of L for antenna frequency detuning when the proposed design is applied to the real notebook computers in practice.

V. CONCLUSION

A compact, printed loop antenna with the dimensions 5 mm × 20 mm only, including the loop radiator and the small antenna ground thereof, for 2.4/5.2/5.8 GHz, tri-band WLAN operation has been presented. The loop structure was small and occupied an area of 4 mm × 15 mm. The quarter-wavelength loop mode was generated with the use of the capacitively-driven feed inserted close to the antenna feed port. In addition, with the incorporation of the matching inductor end-loaded between the loop and the ground, the operating frequencies of the quarter- and the half-wavelength loop modes can be decreased and adjusted for 2.4 and 5.2/5.8 GHz operation. Omnidirectional radiation patterns with good radiation performance over the bands were also obtained. The design footprint is the smallest among those similar notebook computer antennas. Owing to its small lateral length of 20 mm and low profile of 5 mm, the proposed design can be easily embedded in the bezel of the notebook display with possible 4 × 4 multiple transmit/receive antennas integrated for future Gbps communications.

REFERENCES

[1] D. Liu and B. Gaucher, "A triband antenna for WLAN applications," in *IEEE Antennas Propag. Soc. Int. Symp. Dig.*, Columbus, OH, USA, Jun. 2003, pp. 18–21.
[2] C.-M. Su, W.-S. Chen, Y.-T. Cheng, and K.-L. Wong, "Shorted T-shaped monopole antenna for 2.4/5 GHz WLAN operation," *Microw. Opt. Technol. Lett.*, vol. 41, pp. 202–203, May 2004.
[3] D. Liu and B. Gaucher, "A branched inverted-F antenna for dual band WLAN applications," in *IEEE Antennas Propag. Soc. Int. Symp. Dig.*, Monterey, CA, USA, Jun. 2004, pp. 2623–2626.
[4] K.-L. Wong, L.-C. Chou, and C.-M. Su, "Dual-band flat-plate antenna with a shorted parasitic element for laptop applications," *IEEE Trans. Antennas Propag.*, vol. 53, no. 1, pp. 539–543, Jan. 2005.
[5] H. W. Liu, S. Y. Lin, and C. F. Yang, "Compact inverted-f antenna with meander shorting strip for laptop computer WLAN applications," *IEEE Antennas Wireless Propag. Lett.*, vol. 10, pp. 540–543, 2011.
[6] C.-T. Lee and S.-W. Su, "Tri-band, stand-alone, PIFA with parasitic, inverted-L plate and vertical ground wall for WLAN applications," *Microw. Opt. Technol. Lett.*, vol. 53, pp. 1797–1803, Aug. 2011.
[7] J. Yeo, Y. J. Lee, and R. Mittra, "A novel dual-band WLAN antenna for notebook platforms," in *IEEE Antennas Propag. Soc. Int. Symp. Dig.*, Monterey, CA, USA, Jun. 2004, pp. 1439–1442.
[8] L. C. Chou and K. L. Wong, "Uni-planar dual-band monopole antenna for 2.4/5 GHz WLAN operation in the laptop computer," *IEEE Trans. Antennas Propag.*, vol. 55, no. 12, pp. 3739–3741, Dec. 2007.
[9] C.-T. Lee and K.-L. Wong, "Uniplanar printed coupled-fed PIFA with a band-notching slit for WLAN/WiMAX operation in the laptop computer," *IEEE Trans. Antennas Propag.*, vol. 57, no. 4, pp. 1252–1258, Apr. 2009.
[10] K.-B. Kim, H.-K. Ryu, and J.-M. Woo, "Compact wideband folded monopole antenna coupled with parasitic inverted-L element for laptop computer applications," *Electron. Lett.*, vol. 47, pp. 301–303, Mar. 2011.
[11] L. Guo, Y. Wang, Z. Du, Y. Gao, and D. Shi, "A compact uniplanar printed dual-antenna operating at the 2.4/5.2/5.8 GHz WLAN bands for laptop computers," *IEEE Antennas Wireless Propag.*, vol. 13, pp. 229–232, 2014.
[12] C.-Y.-D. Sim, C.-C. Chen, X. Y. Zhang, Y.-L. Lee, and C.-Y. Chiang, "Very small-size uniplanar printed monopole antenna for dual-band WLAN laptop computer applications," *IEEE Trans. Antennas Propag.*, vol. 65, no. 6, pp. 2916–2922, Jun. 2017.
[13] C. Sim, H.-Y. Chien, and C.-H. Lee, "Dual-/triple-band asymmetric dipole antenna for WLAN operation in laptop computer," *IEEE Trans. Antennas Propag.*, vol. 61, no. 7, pp. 3808–3813, Jul. 2013.
[14] D. Liu and B. Gaucher, "Performance analysis of inverted-F and slot antennas for WLAN applications," in *IEEE Antennas Propag. Soc. Int. Symp. Dig.*, Columbus, OH, USA, Jun. 2003, pp. 14–17.
[15] C.-M. Su, H.-T. Chen, F.-S. Chang, and K.-L. Wong, "Dual-band slot antenna for 2.4/5.2 GHz WLAN operation," *Microw. Opt. Technol. Lett.*, vol. 35, pp. 306–308, Nov. 2002.
[16] C.-T. Lee, S.-W. Su, S.-C. Chen, and C.-S. Fu, "Low-cost, direct-fed slot antenna built in metal cover of notebook computer for 2.4-/5.2-/5.8-GHz WLAN operation," *IEEE Trans. Antennas Propag.*, vol. 65, no. 5, pp. 2677–2682, May 2017.
[17] S.-W. Su, "Concurrent dual-band six-loop-antenna system with wide 3-dB beamwidth radiation for MIMO access points," *Microw. Opt. Technol. Lett.*, vol. 52, pp. 1253–1258, Jun. 2010.
[18] S.-W. Su, "High-gain dual-loop antennas for MIMO access points in the 2.4/5.2/5.8 GHz bands," *IEEE Trans. Antennas Propag.*, vol. 58, no. 7, pp. 2412–2419, Jul. 2010.
[19] T.-C. Hong and S.-W. Su, "Compact high-gain printed loop-antenna array integrated into a 5-GHz WLAN access point," *Microw. Opt. Technol. Lett.*, vol. 52, pp. 2261–2267, Oct. 2010.
[20] S.-W. Su and T.-C. Hong, "Printed, multi-loop-antenna system integrated into a concurrent, dual-WLAN-band access point," *Microw. Opt. Technol. Lett.*, vol. 53, pp. 317–322, Feb. 2011.
[21] S.-W. Su, "Printed loop antenna integrated into a compact, outdoor WLAN access point with dual-polarized radiation," *Prog. Electromagn. Res. C*, vol. 19, pp. 25–35, 2011.
[22] S.-W. Su and C.-T. Lee, "Low-cost dual-loop-antenna system for dual-WLAN-band access points," *IEEE Trans. Antennas Propag.*, vol. 59, no. 5, pp. 1652–1659, May 2011.
[23] S.-W. Su, "Compact four-loop-antenna system for concurrent, 2.4- and 5-GHz WLAN operation," *Microw. Opt. Technol. Lett.*, vol. 56, pp. 208–215, Jan. 2014.
[24] H. Morishita, Y. Kim, and K. Fujimoto, "Design concept of antennas for small mobile terminals and the future perspective," *IEEE Antennas Propag. Mag.*, vol. 44, no. 5, pp. 30–34, Oct. 2002.
[25] T. Adachi, A. Hirata, and T. Shiozawa, "Folded-loop antennas for handset terminals at the 2.0-GHz band," *Microw. Opt. Technol. Lett.*, vol. 36, pp. 376–378, Mar. 2003.
[26] B. Jung, H. Rhyu, Y.-J. Lee, F. J. Harackiewicz, M.-J. Park, and B. Lee, "Internal folded loop antenna with tuning notches for GSM/GPS/DCS/PCS mobile handset applications," *Microw. Opt. Technol. Lett.*, vol. 48, pp. 1501–1504, Aug. 2006.
[27] K. L. Wong and C. H. Huang, "Printed loop antenna with a perpendicular feed for penta-band mobile phone application," *IEEE Trans. Antennas Propag.*, vol. 56, no. 7, pp. 2138–2141, Jul. 2008.
[28] Y.-W. Chi and K.-L. Wong, "Compact multiband folded loop chip antenna for small-size mobile phone," *IEEE Trans. Antennas Propag.*, vol. 56, no. 12, pp. 3797–3803, Dec. 2008.
[29] Y.-W. Chi and K.-L. Wong, "Quarter-wavelength printed loop antenna with an internal printed matching circuit for GSM/DCS/PCS/UMTS operation in the mobile phone," *IEEE Trans. Antennas Propag.*, vol. 57, no. 9, pp. 2541–2547, Sep. 2009.
[30] K.-L. Wong and Z.-H. Feng, "On-frame dual-loop antenna with narrow ground clearance for the 2.4/5.2/5.8-GHz WLAN operation in the smartphone," *Microw. Opt. Technol. Lett.*, vol. 58, pp. 1480–1485, Jun. 2016.
[31] ANSYS Inc. *ANSYS HFSS*. Accessed: Jan. 2018. [Online]. Available: http://www.ansys.com/Products/Electronics/ANSYS-HFSS
[32] K.-L. Wong and S.-C. Chen, "Printed single-strip monopole using a chip inductor for penta-band WWAN operation in the mobile phone," *IEEE Trans. Antennas Propag.*, vol. 58, no. 3, pp. 1011–1014, Mar. 2010.
[33] SATIMO. *SG 64*. Accessed: Jan. 2018. [Online]. Available: http://www.mvg-world.com/en/products/field_product_family/antenna-measurement-2/sg-64
[34] J. Volakis, *Antenna Engineering Handbook*, 4th ed. New York, NY, USA: McGraw-Hill, 2007, ch. 6, pp. 16–19.
[35] C. A. Balanis, *Antenna Theory: Analysis and Design*, 3rd ed. New York, NY, USA: Wiley, 2012, ch. 2.

SAOU-WEN SU (S'05–M'08–SM'14) received the B.S., M.S., and Ph.D. degrees in electrical engineering from National Sun Yat-sen University, Kaohsiung, Taiwan, in 2001, 2003, and 2006, respectively. From 2006 to 2008, he was with the Technology Research and Development Center, Lite-On Technology Corporation, Taipei, Taiwan, where he was with the Network Access Strategic Business Unit from 2008 to 2012. He built up the first Antenna Design Team at the corporate of the Lite-On Technology Corporation, where he contributed numerous cutting-edge designs to the company's ODM projects, including enterprise/SMB access point, router, Bluetooth headset, home entertainment device, media box, and RF module. Since 2012, he has been with the ASUSTek Computer Inc., Taipei, where he is currently the Leader of the Antenna Design Department, Advanced EM and Wireless Communication Research and Development Center, for all notebook, 2-in-1 PC, and smartwatch antenna design projects, including Zenbook, Zenbook Flip, ZenWatch, and ZenFone 2. He has authored or co-authored 100 refereed journal papers, among which 13 papers are single-author papers conducted on his own and 27 international conference articles. He holds 48 U.S. and 56 Taiwan patents granted with many patents pending. He is listed in the *Who's Who in the World 2014*. He served as a member of the judge panel for the 2014 and 2016 National Terminal Antenna Design Competition organized by the Taiwan Ministry of Economics. He received the one-year full-time School Study Exchange Program Scholarship to The University of Auckland, New Zealand, from the Asian 2000 Foundation in 1998. He received the Outstanding Technical Achievement Award from the IEEE Tainan Section in 2016. He is a Senior Member of the IEEE Antennas and Propagation Society and a Life Member of the Institute of Antenna Engineers of Taiwan. He served or currently serves as a reviewer for the IEEE TRANSACTIONS ON ANTENNAS AND PROPAGATION, the IEEE ANTENNAS AND WIRELESS PROPAGATION LETTERS, the *Electronic Letters*, the *IET Microwave, Antennas and Propagation*, and the *Progress in Electromagnetic Research* journals.

CHENG-TSE LEE (S'08–M'10) was born in Yilan, Taiwan, in 1983. He received the B.S. degree in electronic engineering from the National Changhua University of Education, Changhua, Taiwan, in 2005, and the M.S. and Ph.D. degrees in electronic engineering from National Sun Yat-sen University, Kaohsiung, Taiwan, in 2007 and 2010, respectively. From 2010 to 2014, he was with the Network Access Strategic Business Unit, Lite-On Technology Corporation, Taipei, Taiwan, where he contributed numerous cutting-edge antenna designs to the company's ODM and research projects, including enterprise/SMB access point, router, wireless speaker, RF module, and smart antenna system. Many customized antenna designs were successfully applied to these products. Since 2014, he has been with the Advanced EM and Wireless Communication Research and Development Center, Antenna Design Department, ASUSTek Computer Inc., Taipei, where he is dedicated to creating many advanced RF antenna designs for Zenbook and Zenbook Flip with fully metallic industry design. He and his team received the Honorable Mention for the 2006, 2007, and 2008 National Terminal Antenna Design Competition organized by the Taiwan Ministry of Economics.

SHU-CHUAN CHEN (M'13) received the B.S. and M.S. degrees in electrical engineering from the Chung Cheng Institute of Technology, National Defense University, Taoyuan, Taiwan, in 1998 and 2004, respectively, and the Ph.D. degree in electrical engineering from National Sun Yat-sen University, Kaohsiung, Taiwan, in 2012. Since 2012, she has been an Assistant Professor with the Department of Electrical and Electronic Engineering, Chung Cheng Institute of Technology, National Defense University, where she became an Associate Professor in 2016. She has authored over 20 refereed SCI journal papers and numerous international conference articles. She also holds over 20 patents, including U.S., Taiwan, and China patents. Her main research interests are in internal antennas for mobile communication devices.